A mathematical model for the analysis of timing behaviors

Takayuki Hasegawa

University of Toyama

Abstract

In this study, the author developed a fundamental theory of interval timing behavior, inspired by the learning-to-time (LeT) model and the scalar expectancy theory (SET) model. The proposed model of timing behavior comprises *clocks*, a *regulator*, a *mixer*, a *response*, and *memory*. This theoretical model was verified by measuring the timing behavior using real animals. In the animal experiment using rats with the peak-interval procedure, the rats were required to press a lever after a certain period of time from a cue tone onset. Numerical values randomly generated by a computer were input to the above theoretical model, and parameters in the model were set so that the correlation coefficient between the theoretical model and the actual frequency distribution curves of lever pressing became higher. The results indicated that the theoretical model well showed "scalar property", in which, even if the length of targeted time in timing behaviors is changed, altered reaction patterns of animals can be superimposed to the original pattern by similarity transformation in the time axis direction. Thus, this model can incorporate "transposition" in psychology (a phenomenon that generalization gradient depends on relative scale) as scalar property. Furthermore, the Akaike information criterion (AIC) values indicated that the current model fit the data better than did the SET model. The present mathematical model with the above characteristics should be an important key in elucidating neurophysiological mechanisms of time perception.

1 Introduction

"What is time?" Among the innumerable, difficult problems as yet unsolved by humans, this may be one of the toughest. The ultimate goal of the author is the mathematical axiomatization of psychological time (subjective time) achieved through an analysis founded on behavioral science. Physicists have long expressed objective time as a real number line. Subsequently, in the last century, objective time was embodied in Minkowski spacetime, a four-dimensional space possessing time as the fourth coordinate, by theorists of relativity. It seems to us, however, that even Zeno's paradoxes, such as "Achilles and the tortoise" and "the arrow," are as yet unsettled (Vlastos 1967, Alper and Bridger 1997). Some of the important open questions that remain are the following: "What is *subjective time* like?"; "How do organisms perceive *time*?"; and "How are organisms' perceptions of *time* reflected in their behavior?" The author must collect facts about the characteristics of subjective time before he can identify its underlying mathematical axioms. The present analysis targets identifying such axioms.

1.1 Time perception and interval timing

Perceived time is also called psychological time, and it is distinct from physically measured time. Unlike most perceptions, which are based on the senses, the perception of time is not associated with specific organs or external stimuli that create an organisms' experiences of

time. Nonetheless, not only multicellular organisms but also single-celled organisms, such as paramecia and the true slime mould *Physarum polycephalum*, have time perception (Saigusa et al. 2008).

Interval timing is based on time perception. The mechanisms of circadian timing and millisecond timing have been clarified, to some extent. Interval timing, however, differs from circadian timing and millisecond timing in its precision. Interval timing is less precise than either of the other two types of timing: it is accurate only to within a wide seconds-to-minutes-to-hours range, while circadian timing is precise to within a narrow range of around twenty-four hours, and millisecond timing is of a mixed precision that lies within the subsecond range (Buhusi and Meck 2005). Given this difference in precision, it is likely that the mechanism underlying interval timing differs from those underlying these other two forms of timing.

In the current study, fixed interval (FI) schedules of reinforcement were used to study interval timing. With FI schedules, only the first response that occurs after a fixed duration is reinforced. To better study the full course of responding over time, Roberts (1981) invented the peak-interval (PI) procedure. The PI procedure includes both FI trials and probe trials. In probe trials no reinforcement is provided, and the length of the trial greatly exceeds the length of the intervals used during the FI trials. Interval timing is often investigated through use of the PI procedure (See Fig. 9 on page 24 for actual data

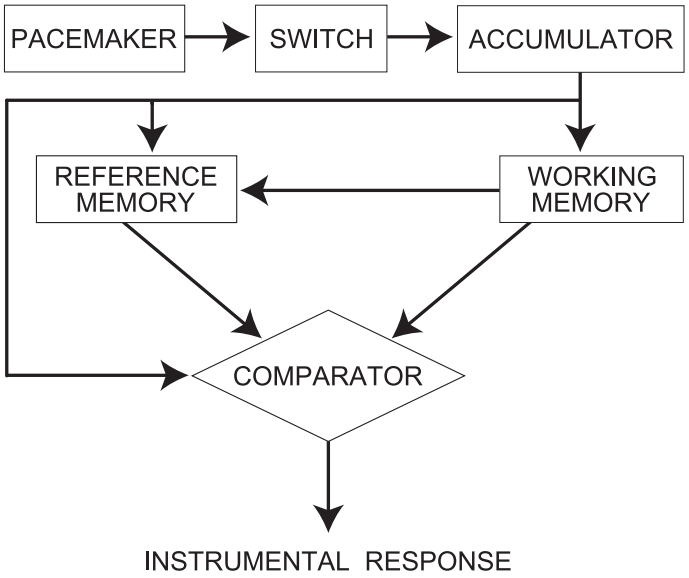

Figure 1: Structure of the scalar expectancy theory (SET) model, updated by Figure 1 in Allman et al. (2014). A pacemaker generates pulses. Pulses are first stored in an accumulator and then stored in the working memory. After reinforcement, the contents of the working memory are transferred to the reference memory. In later trials, previous delay lengths stored in the reference memory are compared with the number in the accumulator, and the ratio of the two numbers determines the subsequent behavior

from my experiment, shown as dots; also see Figure 2 in Church (1984); Zentall 2006)[*1].

1.2 SET and LeT

Investigations of vertebrates' sensitivity to time have culminated in many theories. Among them, the scalar expectancy theory (SET) model and the learning-to-time (LeT) model are mathematically interesting[*2].

Gibbon and his colleagues developed the SET model of timing (Gibbon 1977; Gibbon, Church and Meck 1984). SET is very successful at describing subjective time across many interval lengths. In short, SET provides a cognitive and stochastic account of

[*1]Abbreviations. FI schedule, fixed interval schedule; PI procedure, peak-interval procedure.

[*2]Abbreviations. SET, the scalar expectancy theory; LeT model, the learning-to-time model.

information processing to explain temporal behavior in animals. The components of SET are a pacemaker, a switch, an accumulator, memories, and a comparator, and the model proposes that together these components produce instrumental responses (Fig. 1. See also Figure 1 in Allman et al. (2014) and its detailed neurological review). The explicit solution of a PI procedure is

$$R(t) = a \exp\left\{ -\frac{1}{2} \left(\frac{t - t_0}{b} \right)^2 \right\} + R_0, \tag{1}$$

where $R(t)$ is the operant response function at time t, t_0 is the t-coordinate of the vertex of the graph of $R(t)$, b is the standard deviation, and a and R_0 are parameters. This is a modified version of the density function for the normal distribution.

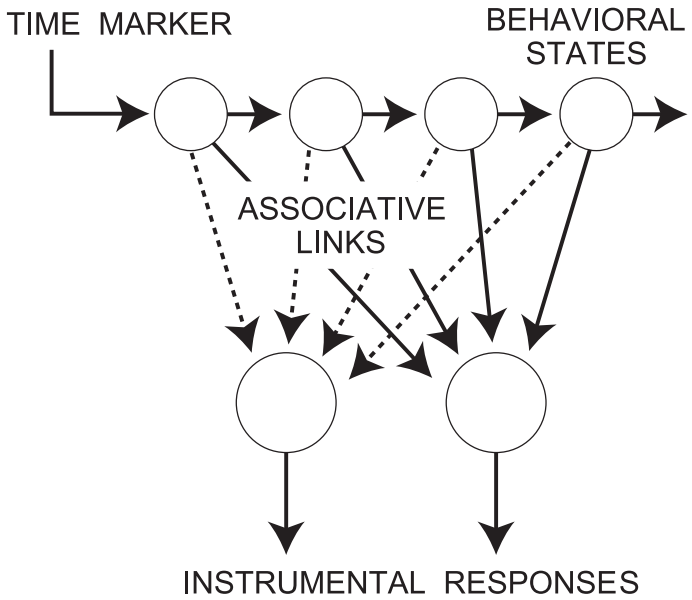

Figure 2: Structure of the learning-to-time (LeT) model. A time marker initiates the activation of behavioral states. These serial states are multiplied by each associative link. The summation of these products determines behavior

Machado developed the LeT model of timing, retaining the basic elements of the behavioral theory-of-timing (BeT) model, which was developed by Killeen and Fetterman (1988; Machado 1997; Machado and Guilhardi 2000; Killeen and Taylor 2000)[*3]. In short, the LeT model is a behavioral and deterministic account of learning formulated to explain temporal behavior in animals. Its components, which include behavioral states and associative links, produce instrumental responses (Fig. 2). The LeT model therefore describes a dynamical system that individuals use to produce temporal behavior.

Both SET and LeT inspired the current author's ambition to create a new theory of timing behavior that is both descriptive and interpretive of quantitative analyses in neuroscience. Although this theory is similar to LeT in several ways, the author hope that, like SET, it will be successful at describing subjective timing behavior across a wide range of interval lengths.

[*3]Abbreviation. BeT, the behavioral theory-of-timing model.

2 A new model of timing behavior

Since mathematics is a deductive system, it is convenient to construct a deterministic model of timing behavior. However, this does not imply that a useful stochastic model of this timing behavior could not be developed.

2.1 Model of clocks; functions $X_n(t)$

Gibbon, Church and Meck (1984) incorporated into SET the assumption that an internal "pacemaker" exists. Machado used clocks modelled by a cascade (stream flow) as "behavioral states" in the LeT model (Machado 1997). My model also assumes the existence of clocks, although I do not yet know how these clocks are related to the organisms' counting-like behaviors (Meck 1996, 2006; Fetterman et al. 1998; Matell and Meck 1999; Staddon and Higa 1999; Grondin 2001; Matell et al. 2003; Clément and Droit-Volet 2006; Saigusa et al. 2008; Beckmann and Young 2009). I am thus willing to consider models that offer precise accounts of specific types of timing behavior as well as those that provide more general accounts of a wider range of timing behaviors.

The cascade model used to create my model of timing behavior is illustrated in Fig. 3. This cascade model is simple, and it has much in common with the cascade model that is part of the LeT model. In my model, the containers are aligned vertically, and each container is analogous to a clock. These clocks each provide information to the organism

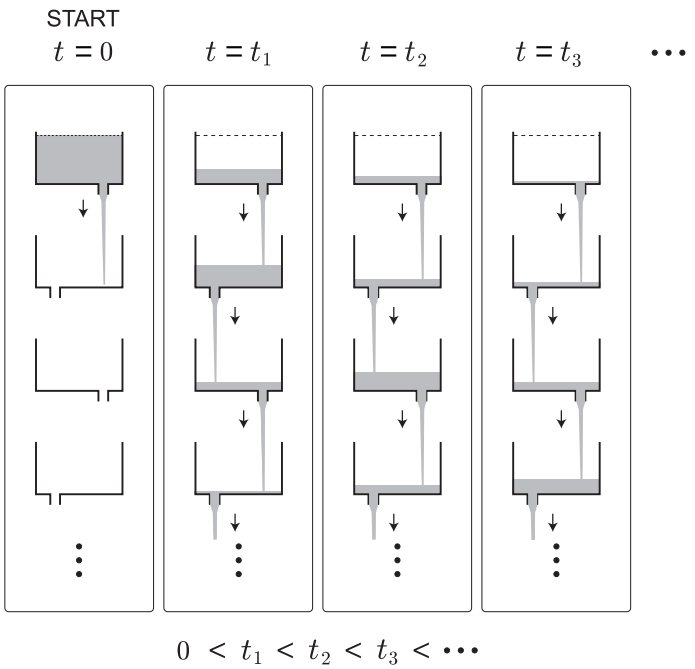

Figure 3: Snapshots of the cascade model used to illustrate the dynamics of clocks. There is a hole in the bottom of each container. At the beginning of a PI trial (represented by the leftmost column in the figure), the top container is filled with water, and the other containers are empty. In this figure, the columns from left to right provide a series of snapshots of the state of the containers as time elapses, and thus the quantity of water in each one changes. The quantity of water in each container may be considered analogous to the amount of influence the associated clock has on the subject's estimate of the length of the interval being timed that has thus far elapsed

about how much of the interval has elapsed, and the "volume" with which a given clock provides this information is equivalent to the amount of water in the corresponding container. I use $X_n(t)$ to denote the amount of water in the nth container ($n = 0, 1, 2, 3, \ldots$), where t ($\geqq 0$) represents the physical time that has elapsed since the onset of the interval being timed. I assume that $X_n(t)$ is differentiable at any time t, and the value of $X_n(t)$ is a nonnegative real number. Let λ be a positive constant. Based on Machado (1997), I propose the following set of differential equations:

$$X_0(0) = 1, \tag{2}$$

$$\frac{d}{dt}X_0(t) = -\lambda X_0(t); \tag{3}$$

$$X_n(0) = 0 \quad (n = 1, 2, 3, \ldots), \tag{4}$$

$$\frac{d}{dt}X_n(t) = \lambda X_{n-1}(t) - \lambda X_n(t) \quad (n = 1, 2, 3, \ldots). \tag{5}$$

Equation (2) is the initial condition of $X_0(t)$, and it expresses the fact that the top container is filled with water at the beginning ($t = 0$) of each trial. Equation (4) is the initial condition of $X_n(t)$ ($n = 1, 2, 3, \ldots$), and it expresses the fact that the other containers are empty at $t = 0$. In Eq. (3), $\frac{d}{dt}X_0(t)$ is the first derivative of $X_0(t)$, and $\frac{d}{dt}X_0(t)$ can be read as the differential coefficient of $X_0(t)$ at time t, which is the rate of change (decrease, in this case) of $X_n(t)$ at time t. Thus, Eq. (3) expresses the fact that water in the top container flows out of that container at a rate proportional to the amount of water left in the container at that time. The positive constant λ, previously defined, is used here as the proportional coefficient in this relation. Take an arbitrary n ($n = 1, 2, 3, \ldots$), and hold it fixed. In Eq. (5), $\frac{d}{dt}X_n(t)$ on the left-hand side can be read as the rate of change of $X_n(t)$ at time t. The term $\lambda X_{n-1}(t)$ on the right-hand side expresses the fact that the nth container receives water at a rate proportional to the amount of water in the $(n-1)$th container at that time, and the term $-\lambda X_n(t)$ on the same side expresses the fact that the nth container loses water at a rate proportional to the amount of water in the nth container at that time. Inductively, the term $\lambda X_{n-1}(t)$

may be read as the rate at which the previous $(n-1)$th container loses water. All the proportional coefficients of the relations described by Eqs. (2)–(5) are identical and are equal to the constant λ.

As can be proven by mathematical induction on n, the solution of Eqs. (2)–(5) is the density function of the Poisson distribution, i.e., the gamma density function:

$$X_n(t) = \frac{\exp(-\lambda t) \cdot (\lambda t)^n}{n!} \quad (n = 0, 1, 2, 3, \ldots). \tag{6}$$

The graph for each n $(n = 0, 1, 2, 3)$ is presented in Fig. 4, using $\frac{1}{\lambda} = 15$ seconds to provide an illustrative example. By differential calculus, we see that $X_n(t)$ has its peak at $t = \frac{n}{\lambda}$ $(n = 0, 1, 2, 3, \ldots)$.

During each trial, the value of λ was determined in some way by the data extracted from *memory*, and after each FI trial ends with reinforcement, the new value of λ is stored in *memory*. This process corresponds to what was called "recalibration" by Killeen (1975; Fetterman and Killeen 1991).

In the present model, I assume that it is necessary to express each instant of time $\frac{n}{\lambda}$ $(n = 0, 1, 2, 3, \ldots)$ with an accompanying span for both before and after that moment $\frac{n}{\lambda}$; note that this spread does *not* indicate an error. This deterministic model differs in this from the stochastic counter model offered by Killeen and Taylor (2000), which used

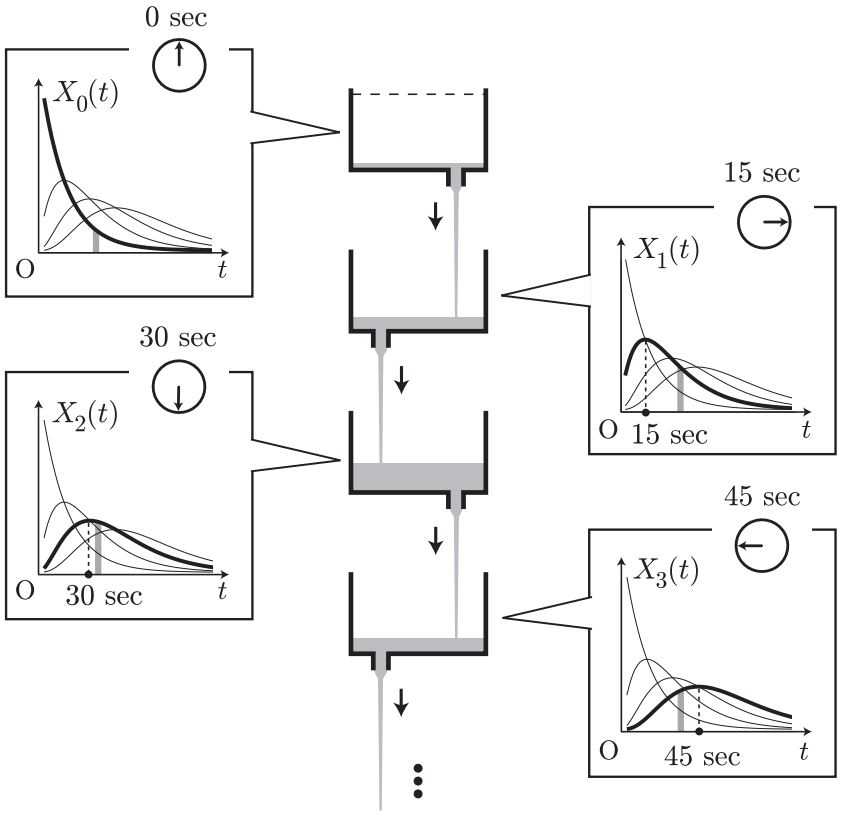

Figure 4: Example of the clocks included in the Poisson decomposition (PD) model. Graphs of $X_n(t)$ $(n = 0, 1, 2, 3)$, plotted with bold lines, show the change in water quantity in the containers after time t, the physical time elapsed since the start of the trial. $X_n(t)$ has its peak at $t = \dfrac{n}{\lambda}$ $(n = 0, 1, 2, 3)$. The peak times in these graphs are examples where $\dfrac{1}{\lambda}$ is arbitrarily set to be 15 (sec)

the cascade as an explanation of the error.

As is mentioned in Dayan and Abbott (2001, p. 34) "even when it successfully describes data, the Poisson model does not provide a mechanistic explanation of neuronal response variability," that is, it is not necessary to find a cascade structure in biological systems. Figure 3 is an abstract example to explan the consecutive reaction, which is widely studied in chemistry. In many applications, the outputs of the model clocks should be replaced by actual output.

2.2 Model of regulator; functions $c_n(s)X_n(t)$

N denotes the total number of sessions, and $m + 1$ denotes the maximal number of clocks used. Mathematically speaking, in the sth session ($s = 1, 2, 3, \ldots, N$), for each n ($n = 0, 1, 2, \ldots, m$), the *regulator* prepares the set of real numbers $c_n(s)$; then it calculates the product $c_n(s)X_n(t)$, amplifying $X_n(t)$ by $c_n(s)$. In other words, the *regulator* assigns weights to the clocks. I assume that the weights $c_n(s)$ are constant within a session. In this regard, the LeT model has the associative strength function $W_n(t)$, which varies within a trial.

During each trial, the set of values of $c_n(s)$ is determined by the data extracted from *memory*, and after each FI trial ends with reinforcement, the new set of values of $c_n(s)$ is stored in *memory*. This process forms an additional component of the "recalibration" process.

2.3 Model of mixer; function $R_s(t)$

I use $R_s(t)$ to denote the psychometric function, the source of the operant response, which is produced by the *mixer*, in the sth session of a trial.

In my model, I define $R_s(t)$ such that

$$R_s(t) = \sum_{n=0}^{m} c_n(s)X_n(t), \tag{7}$$

a linear combination of functions $X_n(t)$ with coefficients $c_n(s)$ $(n = 0,\ 1,\ 2,\ \ldots,\ m)$. For a typical example in which $\dfrac{1}{\lambda} = 15$ seconds, the length of the trial is 90 seconds, and $m = 3$, this becomes

$$R_s(t) = \sum_{n=0}^{3} c_n(s) X_n(t)$$

$$= c_0(s)X_0(t) + c_1(s)X_1(t) + c_2(s)X_2(t) + c_3(s)X_3(t). \tag{8}$$

Please note that $c_n(s)$ is not limited to positive real numbers. Let us go one step further into metaphor. If $c_n(s) > 0$, then at a given time t, the living organism hears its internal nth clock claiming, "*It's time*" (the interval has elapsed), $X_n(t)$, amplified by the rate $c_n(s)$, taken as an activating motive. If $c_n(s) < 0$, then at a given time t the living organism hears its internal nth clock claiming, "*It's not time*," $X_n(t)$, amplified by the rate $|c_n(s)|(= -c_n(s) > 0)$, taken as an inhibitory motive; and, if $c_n(s) = 0$, then the living organism does not hear the nth clock. The term *mixer* is used to designate the component of the model involved in this process, which leads to an automatic summation of $c_n(s)X_n(t)$ $(n = 0, 1, 2, \ldots, m)$.

For any natural number m, the functions $X_n(t)$ $(n = 0, 1,\ 2, \ldots, m)$ are linearly independent, which can be shown mathematically. Therefore, for a given $R_s(t)$, their linear combination in Eq. (7) is unique. At the same time, Eq. (7) can be read as a decomposition of $R_s(t)$ into independent components $X_n(t)$ $(n = 0, 1, 2, \ldots, m)$. Thus, in this study, both my total model and my method of analysis are a Poisson decomposition

(PD)[*4].

In the LeT model (Machado 1997), $R(t)$ is defined as

$$R(t) = A \sum_{n \geqq 1} W_n(t) X_n(t)$$

$$= \sum_{n \geqq 1} \{A W_n(t)\} X_n(t),$$

where $W_n(t)$ is the associative strength function of state n ($n = 1, 2, 3, \ldots$) at time t, and A is a positive constant. Since $AW_n(t) \geqq 0$ for all n and t, the series $R(t)$ contains no negative term. Thus, the LeT model cannot include inhibitive processes that reduce the likelihood that a subject will respond *as if* a particular interval has elapsed. With $X_n(t)$ in my PD model, the notion of clocks is changed from the behavioral states in the LeT model and permits the use of negative terms.

2.4 Model of operant response; function $\overline{\boldsymbol{R_s(t)}}$

In the current study, the value R of a response rate at a unit time is defined as the value of the ratio of the mean number n of responses at the unit time to the maximal mean number n_m of responses per unit time, namely $R = \dfrac{n}{n_m}$. The value of the response rate is nonnegative and does not exceed one; the operant response function $\overline{R_s(t)}$ may be defined

[*4]Abbreviation. PD, Poisson decomposition.

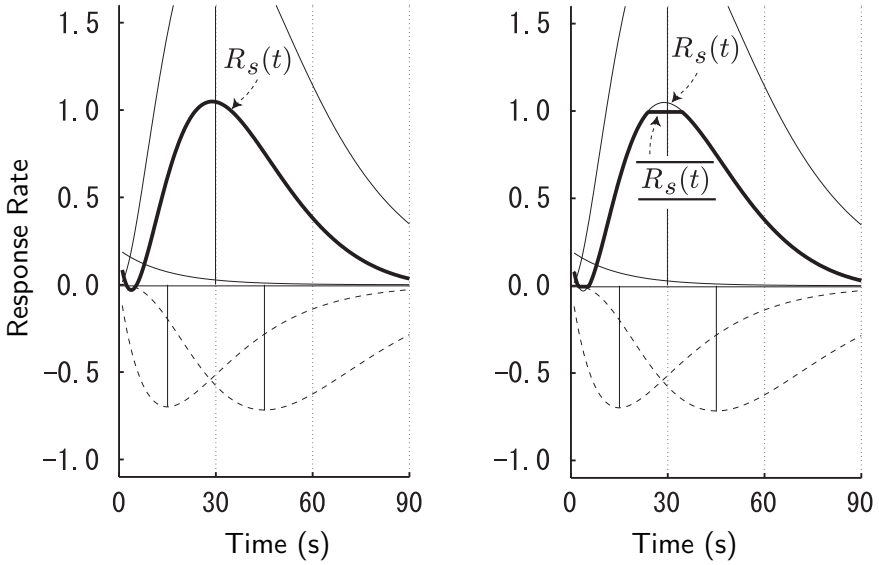

Figure 5: The psychometric function $R_s(t)$, the result of the processes of the *mixer*, becomes $\overline{R_s(t)}$ when it leads to the *response*. $\dfrac{1}{\lambda}$ is assumed to be 15 seconds in the example presented in the figure

as

$$\overline{R_s(t)} = \begin{cases} 1 & (\text{if } R_s(t) > 1), \\ R_s(t) & (\text{if } 0 \leqq R_s(t) \leqq 1), \\ 0 & (\text{if } R_s(t) < 0). \end{cases} \tag{9}$$

Note, for example, the two bold lines in Fig. 5.

Empirical results show that the timing behavior of an animal has a scalar property. This is demonstrated by the fact that the graphs of the timing-response functions for PI schedules in the same animal are almost identical following a linear transformation expressed by some matrix $\begin{pmatrix} a & 0 \\ 0 & b \end{pmatrix}$, where a and b are nonzero real numbers, even if their functions are created under different FI durations in the PI schedule (see Figure 4 in Cheng and Meck (2007) for a superimposition of the graphs obtained from PI schedules

of 18, 36, and 72 seconds. Also see Figure 1 in Oprisan and Buhusi (2013); Figure 2 and 3 in Allman et al. (2014) for human peak-interval timing). The scalar property is one of the starting points of SET (Church 2003; Gibbon 1977). It can be shown mathematically that the system of functions $R_s(t)$ has the scalar property if and only if m does not change and $c_n(s)$ $(n = 0, 1, 2, ..., m)$ do not change their ratio. Generally speaking, the system of $\underline{\overline{R_s(t)}}$ does not have the scalar property, but if $R_s(t) \leqq 1$ in its total domain, which is observed in most cases, then $\underline{\overline{R_s(t)}}$ has the scalar property.

2.5 Total model

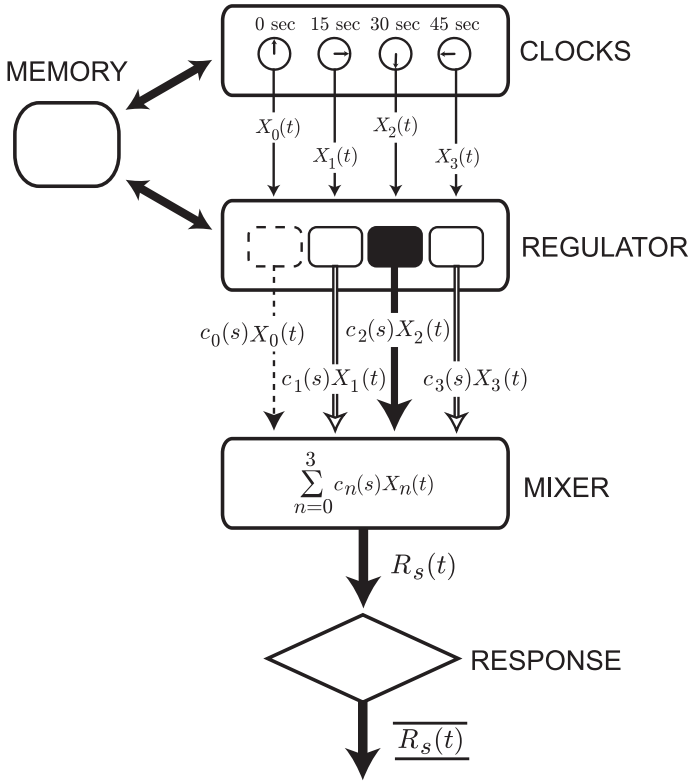

Figure 6: Example ($m = 3$) of my model of the timing of operant responses. Memory contributes to the value the *clocks* assigned to λ, and it influences the *regulator* in fixing $c_n(s)$ $(n = 0, 1, 2, \ldots, m)$. The *mixer* automatically makes $R_s(t)$ the sum of $c_n(s)X_n(t)$ $(n = 0, 1, 2, \ldots, m)$. $R_s(t)$ is the source of $\underline{\overline{R_s(t)}}$, which is produced by the *response*

Figure 6 illustrates an example of my total model of operant responses. The interval $\frac{1}{\lambda}(> 0)$ between the peak times of successive *clocks* will be called "the basic period." The reciprocal, λ, will be called the "speed" of the clock. That is, as the basic period gets smaller, the *clock* ticks at a faster rate. On the other hand, as the basic period increases, the *clock* ticks at a slower rate.

My model assumes that *memory* contributes to the process through which *clocks* set λ to a suitable value; this is based on the length of the FI presented in the early trials of the experiment. *Memory* sends the information about λ to the *clocks*, and *memory* can recalibrate the value after experiencing additional FI trials. My typical $\frac{1}{\lambda}$ setting in the examples in the figure is 15 seconds; in other words, each clock has a length that is 15 seconds longer than the preceding clock.

Memory also contributes to the process through which the *regulator* sets $c_n(s)$ $(n = 0, 1, 2, \ldots, m)$. An example of $R_s(t)$ is presented in the left-hand panel of Fig. 5. In the figure, the coefficients $c_0(s)$ and $c_2(s)$ are positive, because the graphs of $c_0(s)X_0(t)$ and $c_2(s)X_2(t)$, having peak times of 0 $\left(= \frac{0}{\lambda}\right)$ seconds and 30 $\left(= \frac{2}{\lambda}\right)$ seconds, respectively, are located above the horizontal axis. The coefficients $c_1(s)$ and $c_3(s)$ are negative, because the graphs of $c_1(s)X_1(t)$ and $c_3(s)X_3(t)$, having peak times of 15 $\left(= \frac{1}{\lambda}\right)$ seconds and

45 $\left(= \frac{3}{\lambda}\right)$ seconds, respectively, are located below the horizontal axis. In this example, clocks $X_1(t)$ and $X_3(t)$ may be used in the *mixer* for judging, *"It is not 30 seconds yet"* and *"It is not 30 seconds anymore,"* at strengths $|c_1(s)|$ and $|c_3(s)|$, respectively.

The basic idea of the function of the *mixer*, the simple mathematical summation, is similar to that of the generalization gradients and the peak shift by Spence (1937; Mazur 2006). Figure 7 shows a simplified chart of a peak shift.

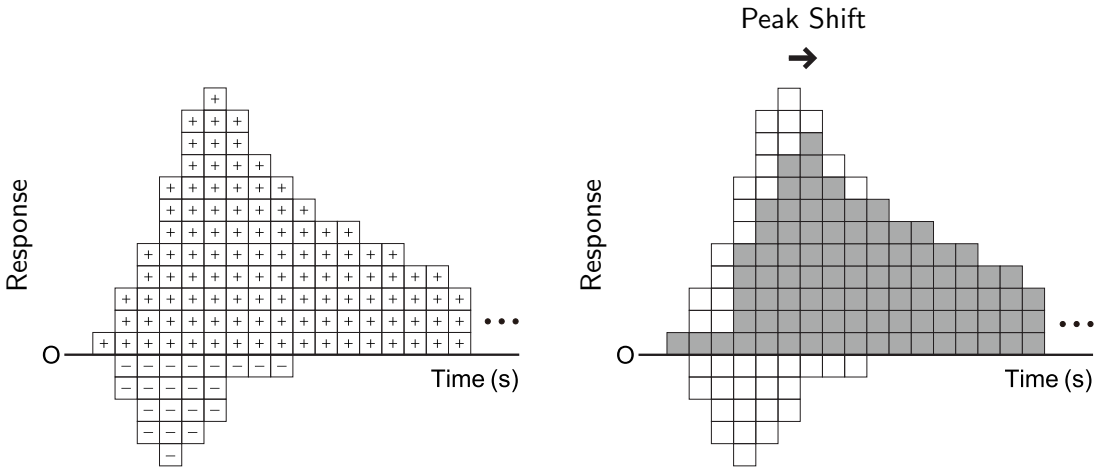

Figure 7: Simplified discrete explanation of a peak shift. The peak time moves as a result of mathematical summation. The grey boxes are the result of the white boxes below the horizontal axis $\boxed{-}$ being subtracted from the white boxes above the horizontal axis $\boxed{+}$

Some examples of peak shifts in my study are shown in Fig. 8. Superposition, as described by Kirkpatrick-Steger et al. (1996; Killeen and Taylor 2000) is different from the process that I am proposing because functions are added in PD, but in superposition, the maximal function is selected.

Through use of the *regulator*, a living organism tries to get better weights, i.e., a set of $c_n(s)$ $(n = 0, 1, 2, 3, \ldots, m)$ that are better for its strategy.

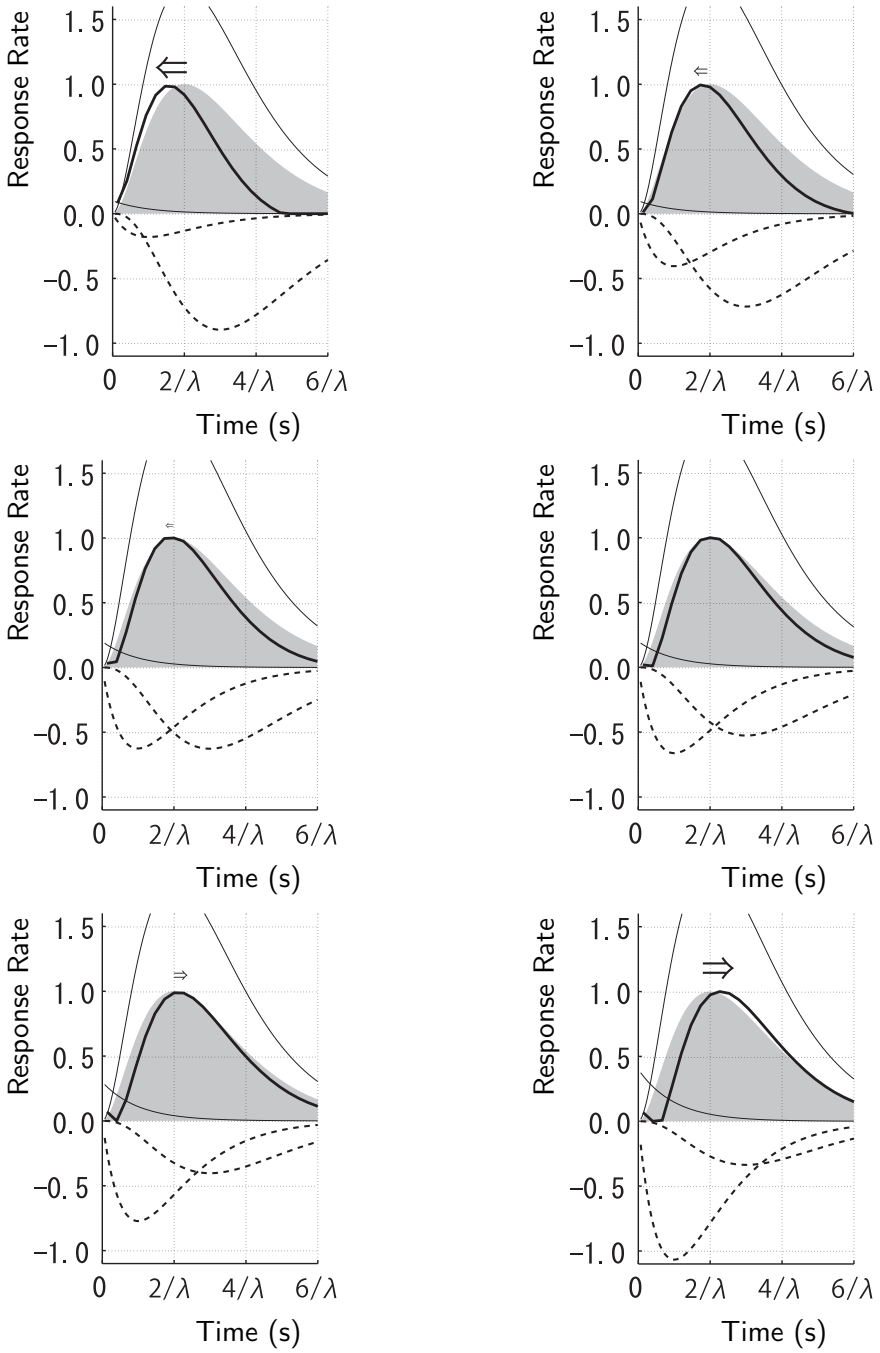

Figure 8: Different possible weights of $c_n(s)$ $(n = 0, 1, 2, 3)$ and the corresponding peak shifts. In each panel, the bold curve is the graph of $\overline{R_s(t)}$, where $R_s(t) = c_0(s)X_0(t) + c_1(s)X_1(t) + c_2(s)X_2(t) + c_3(s)X_3(t)$. The shaded portion is for reference, and it expresses $\dfrac{1}{X_2\left(\frac{2}{\lambda}\right)}X_2(t)$, that is $\dfrac{e^2}{2}X_2(t)$. The two thin curves are the graphs of $c_0(s)$ (near the horizontal line 0.0) and $c_2(s)$ (above, its top is outside the range presented in the figure). The two broken curves are the graphs of $c_1(s)X_1(t)$ (left) and $c_3(s)X_3(t)$ (right), whose ratio determines the shape of $\overline{R_s(t)}$

3 Materials and methods

3.1 Animals

Twelve experimentally naïve male Wistar rats (Cr1j; Japan Charles River Laboratories, Yokohama, Japan) about 15 weeks of age were used: [group RatsA] RatA1, RatA2, ..., RatA6; [group RatsB] RatB1, RatB2, ..., RatB6.

The rats were housed individually in an environment with a constant room temperature of 23°C. The ratio of light to darkness was 1 : 1. Lights were on from 8 a.m. to 8 p.m.; otherwise, lights were off. Each animal received 1.35 g (= 30 × 45 mg) of Dustless Precision Pellets (F0165; Bio-Serv, NJ, USA) as reinforcers during the experiment. Additional food (CE-2; Clea Japan, Inc., Tokyo, Japan) and water were provided in the subjects' home cages after the daily experimental session; this diet was presented at the same time each day. This post-session feeding was the amount necessary to maintain each subject at 85% of their free-feeding weight.

3.2 Apparatus

Each of the 6 operant chambers (25 cm × 30 cm × 30 cm) was equipped with a pellet dispenser, a lever, a light, and a charge-coupled device (CCD) camera. The front and back walls were aluminum; the side walls and the ceiling were transparent acrylic. The

floor was made up of 16 parallel stainless steel bars.

The pellet dispenser (PD-50; Oharamedic, Tokyo, Japan) delivered 45 mg pellets into a food cup, which was attached to the front wall near the floor grid. The lever (H23-17RA; Coulbourn, PA, USA) was located in the front wall about 2.5 cm above the floor grid. A one-watt light was located on the ceiling. The CCD camera (KCB-401P; Mother Tool, Nagano, Japan) was located near the light. The behavior of the rats was monitored remotely by a liquid crystal display placed outside the experiment room. Each chamber was located inside a ventilated box (40 cm $\times$ 62 cm $\times$ 46 cm) that was used for sound and light reduction. One computer (Endeavor VZ-4000; EPSON, Tokyo, Japan) controlled all the experimental events and recorded the times at which each event and response occurred for each individual in each experiment. Another computer (VAIO PCV-RX62K; SONY, Tokyo, Japan), which was connected to audio amplifiers, produced tone stimuli: pulses of 2000 Hz, on/off every 250 ms (i.e., 4 Hz) and at 80 dB.

3.3 Procedure

Let PI-T denote a PI procedure of T seconds, where T = 20, 30, and 45. After lever-pressing was shaped in each subject, the rats were exposed to the PI procedures listed in Table 1.

Each FI trial started with a continuous tone, and the rat received a pellet reinforcer

Table 1: Duration of PI to which RatsA and RatsB were exposed

Session	1–30	31–40	41–50	51–60	61–70
RatsA	PI-30	PI-20	PI-30	PI-45	PI-30
RatsB	PI-30	PI-45	PI-30	PI-20	PI-30

the first time it pressed the lever while $T < t < 3T$, for the specified T. The continuous tone stopped when the rat received the reinforcement, and this was followed by a silent intertrial interval (ITI) of T seconds[*5]. If the rat did not respond while $T < t < 3T$, then a silent ITI of T s was presented without reinforcement. During the probe trials, the tone stimulus lasted $3T$ s and was followed by a silent ITI of T s.

One session consisted of 100 FI trials and 30 probe trials. The order was pseudorandom; the initial 10 trials were FI schedules, and the remaining 120 trials consisted of 30 units of four trials each, where each unit included one probe trial and three FI trials in random order. One experimental session occurred each day for 70 days.

3.4 Data analysis

The analysis was based on the data from all the probe trials, i.e., non-food cycles, in the 21st through 70th sessions. The mean and individual response rates during the initial $3T$ seconds of each session were fit with the explicit solutions: Eq. (1) for SET and Eq. (9) (with Eq. (8)) for the Poisson decomposition.

[*5]Abbreviation. ITI, intertrial interval.

4 Results

4.1 Fit by Pearson's correlation coefficient and AIC

The Akaike information criterion (AIC) is defined to be

$$\text{AIC} = -2\ln(\text{maximum likelihood}) + 2(\text{number of adjusted parameters}).$$

This criterion indicates which of two models best describes a given data set, based on both how well it accounts for the variation in the data and on how few free parameters it has; if a model has a smaller AIC, then it is considered to be the better model based on these two criteria (Akaike 1974)[*6].

I took some steps to reduce the number of free parameters in Eq. (7) and therefore to reduce the value of its AIC. To this end, my standard setting was $m = 3$, which incorporated into the model the assumption that the rats had used the clocks $X_0(t)$, $X_1(t)$, $X_2(t)$, and $X_3(t)$. In my first model for each session s, there were five free parameters: λ, $c_0(s)$, $c_1(s)$, $c_2(s)$, and $c_3(s)$.

I calculated Pearson's product-moment correlation coefficient (r) in addition to the AIC and used both these values to aid in identifying the model that best accounted for the data. An example using the same data set and the best-fitting functions based on SET and the Poisson decomposition are shown in Fig. 9.

[*6]Abbreviation. AIC, the Akaike information criterion.

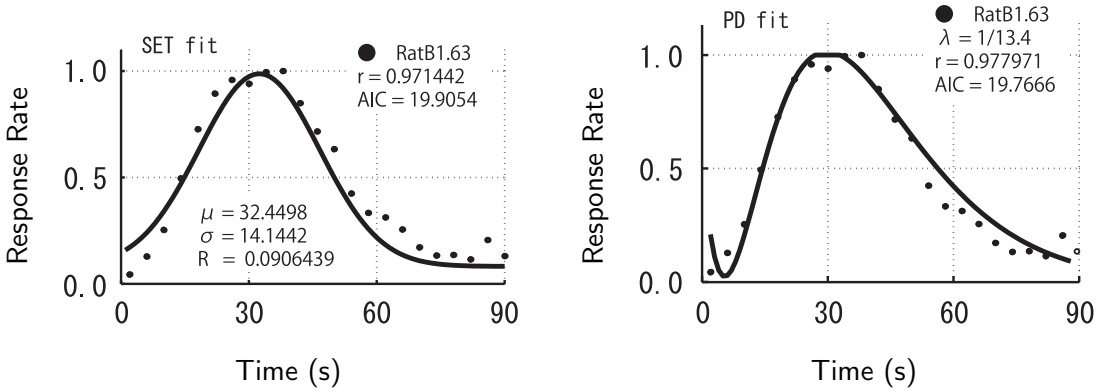

Figure 9: Examples of the fit with SET and with PD for the data from session 63 for RatB1. Rate of response $R(t)$ or $\overline{R_{63}(t)}$ is plotted on the vertical axis. The time t since the onset of the stimulus is plotted on the horizontal axis. Dots represent the mean rate every four seconds. The correlation coefficients (r) of these fits are 0.971 (SET) and 0.978 (PD), the AIC values are 19.91 (SET) and 19.77 (PD). SET and PD have similar values of r and AIC; both of them fit well, and they are almost equally good as mathematical models for this data set, even though I can easily observe a difference in the shapes of the curves

In Fig. 10, the frequency distributions of the Pearson's correlation coefficients (r) for the fits for each session for SET and PD are presented. The judgement of AIC values for this data set is shown on Table 3, and it will be discussed in Section 5.7.

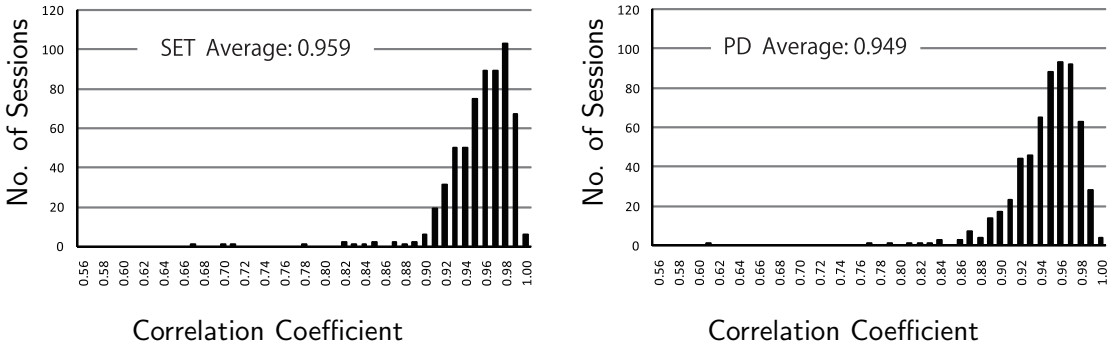

Figure 10: Frequency distribution of the correlation coefficients during the 600 sessions of data collection. The left panel is the frequency distribution for the correlation coefficients for the fits for SET, and the right panel are the same values for the fits for PD. The mean coefficients were 0.959 (SET) and 0.949 (PD). The method used to calculate these means is described in the appendix

4.2 Basic period of clocks

Fitting the PD model to these data allowed the identification of the basic period $\frac{1}{\lambda}$ (s) of the clocks that, according to the proposed model, form part of the process that the subjects used to time the interval. The basic period $\frac{1}{\lambda}$ calculated for each session is presented in Fig. 11, and the means of $\frac{1}{\lambda}$ are shown in Figures 12.

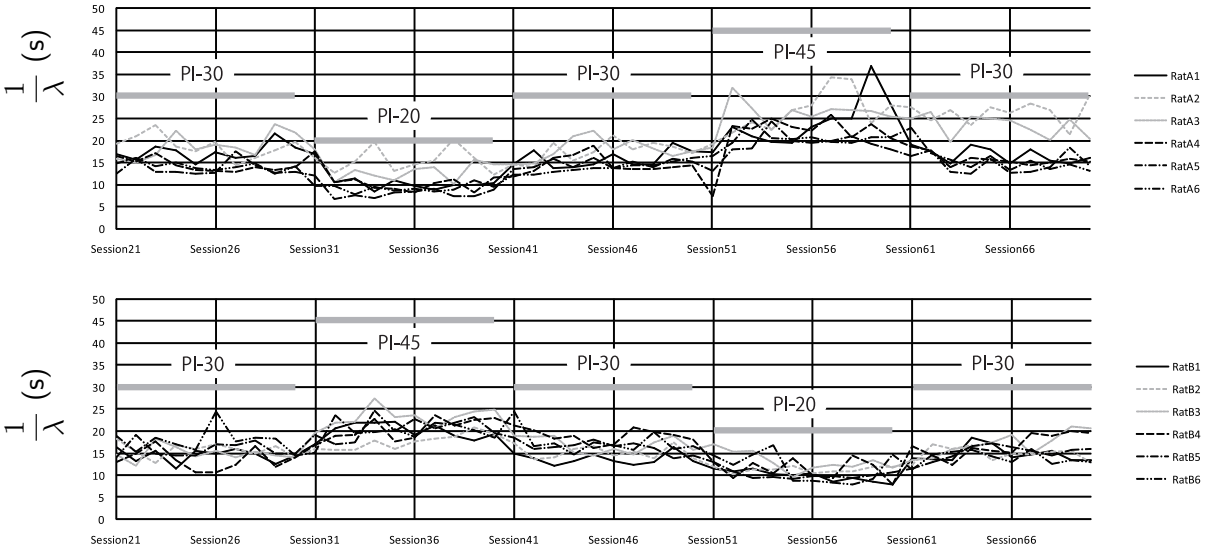

Figure 11: Basic clock periods $\frac{1}{\lambda}$ (s) for each of the 12 rats for each of the 21st to 70th sessions

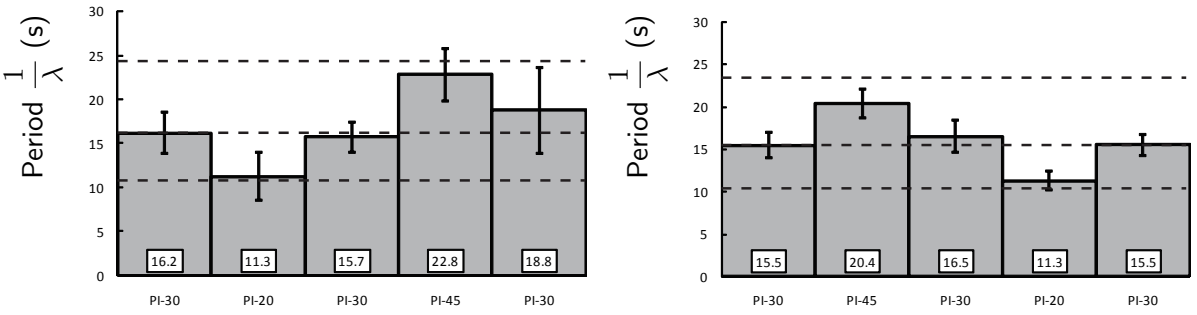

Figure 12: Mean basic clock period $\frac{1}{\lambda}$ (s), by PI length. Error bars present the standard deviations. Broken lines indicate $\frac{3}{2} \cdot \frac{1}{\lambda_0}$, $\frac{1}{\lambda_0}$, and $\frac{2}{3} \cdot \frac{1}{\lambda_0}$, where $\frac{1}{\lambda_0}$ is the basic period of the first PI-30 in sessions 21 through 30. The left and right panels present these values for groups RatsA and RatsB, respectively

4.3 Coefficients identified by Poisson decomposition

After fitting the PD model, the coefficients $c_n(s)$ ($n = 0, 1, 2, 3$; $s = 21, 22, 23, \ldots, 70$) were extracted from the data. An example of a typical graph of $c_n(s)$ ($n = 0, 1, 2, 3$) is shown in Fig. 13.

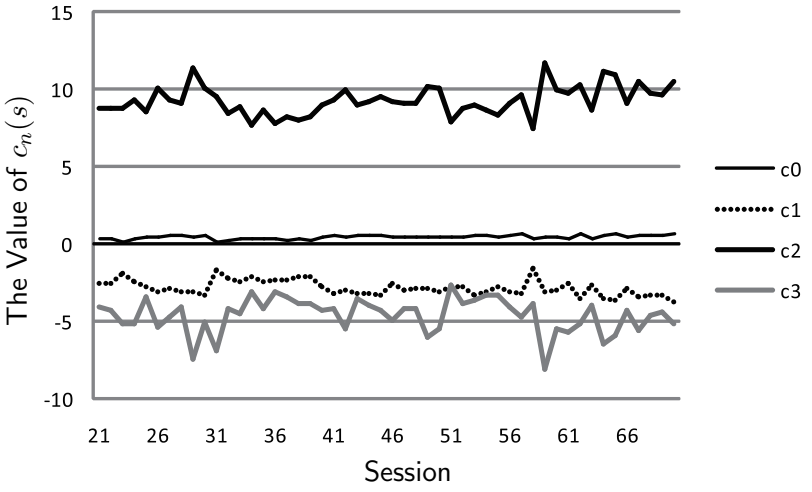

Figure 13: Coefficient $c_n(s)$ for RatA1. $c0$, $c1$, $c2$, and $c3$ are the abbreviations of $c_0(s)$, $c_1(s)$, $c_2(s)$, and $c_3(s)$, respectively

An example of the means of $c_n(s)$ with the same PI length and in the order in which the sessions were presented is shown in Fig. 14.

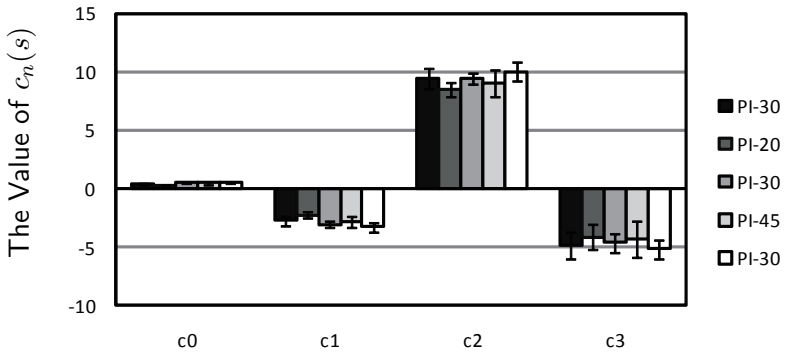

Figure 14: Means of coefficient $c_n(s)$ with standard deviations for RatA1

The means and standard deviations of the $c_n(s)$ are shown in Table 2.

Table 2: The means and standard deviations of the coefficients $c_n(s)$ for all 12 rats

mean	$c_0(s)$	$c_1(s)$	$c_2(s)$	$c_3(s)$
RatA1	0.46	−2.81	9.28	−4.60
RatA2	0.34	−2.11	9.02	−5.45
RatA3	0.57	−3.22	9.98	−5.17
RatA4	0.50	−2.80	8.25	−3.09
RatA5	0.50	−2.81	8.57	−3.51
RatA6	0.49	−2.89	8.68	−3.56
RatB1	0.29	−1.30	5.15	−0.57
RatB2	0.40	−2.29	7.23	−2.28
RatB3	0.47	−2.82	8.92	−4.06
RatB4	0.29	−1.81	7.67	−3.54
RatB5	0.39	−2.50	8.37	−3.62
RatB6	0.32	−2.24	8.15	−3.65

S.D.	$c_0(s)$	$c_1(s)$	$c_2(s)$	$c_3(s)$
RatA1	0.13	0.49	0.93	1.12
RatA2	0.13	0.64	1.13	1.77
RatA3	0.12	0.48	1.16	1.57
RatA4	0.21	0.64	1.17	1.37
RatA5	0.21	0.78	0.97	0.89
RatA6	0.18	0.53	0.90	1.00
RatB1	0.17	0.84	1.12	0.95
RatB2	0.15	0.78	1.61	1.60
RatB3	0.15	0.58	1.22	1.50
RatB4	0.11	0.59	0.87	1.13
RatB5	0.12	0.47	1.01	1.09
RatB6	0.12	0.56	1.05	1.38

5 Discussion 1

Since Yi (2007) has already compared the SET and the LeT models in terms of goodness of fit and complexity, and has concluded that both models do equally well, I will not further consider the LeT model.

5.1 Model of clocks; functions $X_n(t)$

Generally speaking, it is possible that $\frac{d}{dt}X_0(t)$ is not a proportional function of $X_0(t)$. It may be another function, such as $\frac{d}{dt}X_0(t) = -\lambda \{X_0(t)\}^\alpha$ ($\alpha > 0$ and $\alpha \neq 1$; for example, $\alpha = \frac{1}{2}$ by Bernoulli), $\frac{d}{dt}X_0(t) = -\lambda \ln \{X_0(t) + 1\}$, or other possibilities. Moreover, $\frac{d}{dt}X_0(t)$ may depend not only on the amount of water in the container used in the model but also on the size and shape of the hole, as well as on the shape of the container. In fact, there exist many options. Nevertheless, I assumed simply that $\frac{d}{dt}X_0(t)$ depends only on the amount of water $X_0(t)$, and that $\frac{d}{dt}X_0(t)$ is proportional to $X_0(t)$. Additionally, I assumed simply that $\frac{d}{dt}X_n(t)$ depends only on $X_{n-1}(t) - X_n(t)$ and that $\frac{d}{dt}X_n(t)$ is proportional to $X_{n-1}(t) - X_n(t)$ (for any $n = 1, 2, 3, \ldots$) with the same proportional coefficient λ. The reasons for my choice are as follows:

(i) The set of Eqs. (3) and (5) is simple.

(ii) The solutions of the differential equations are gamma density functions whose peak times are equidistant.

I note that gamma density functions are also the foundation of the behavioral theory-of-timing (BeT) stochastic counter model.

5.2 Model of regulator; functions $c_n(s)X_n(t)$

I assumed that the $c_n(s)$ are constant even within sessions. Examining the dynamical fit for the $c_n(s)$ on s is an appropriate and important project for future studies of learning.

5.3 Model of the mixer; function $R_s(t)$

In the case of $c_n(s) = 0$, the living organism hears nothing from the nth clock. If it does not use the clock $X_n(t)$, then I can reduce the AIC value of PD by up to 2 for each n.

If I let

$$R_s(t) = \sum_{n=0}^{m} c_n(s)X_n(t) + R_0,$$

using constant R_0, then R_0 should be 0. The reason is as follows: in the trial interval $0 \leqq t \leqq t_1$, if $t_1 \to +\infty$ and $t \to +\infty$, then $R_s(t) \to 0$; i.e., if a probe trial lasts too long, then the rat will no longer respond at all by the end of the trial.

5.4 Model of operant response; function $\overline{\underline{R_s(t)}}$

In my model, the equation $\overline{\underline{R_s(t)}} = R_s(t)$ holds when $0 \leqq R_s(t) \leqq 1$, but the function $\overline{\underline{R_s(t)}}$ could be defined as another function, depending on the "hardware," such as an animal's motor system.

5.5 Basic speed of clocks

In a PI-30 schedule, for example, if $\dfrac{1}{\lambda} = 15$ (s), then I may say, roughly, that a rat times the interval of 30 s by using the 15 s and 45 s clocks for inhibition, in addition to the 30 s main clock.

5.6 Coefficients by Poisson decomposition

In Sections 2.2 and 5.2, I noted that the weights $c_n(s)$ are assumed to be constant within a session. From Table 2, moreover, I may assume that the values of $c_0(s)$, $c_1(s)$, $c_2(s)$, and $c_3(s)$ are stable against changes in the FI length, and that they are almost constant in each rat from the 21st to the 70th sessions. This implies that the rats cope with the change in the FI length primarily by changing the basic period of their clocks. The weights of $c_0(s)$, $c_1(s)$, $c_2(s)$, and $c_3(s)$ express the organism's proper relative use of clocks $X_0(t)$, $X_1(t)$, $X_2(t)$, and $X_3(t)$, and the weights are almost fixed, which implies a transposition.

Table 3: The number of sessions for which each of the three models produced AIC values that were, among the three models compared, the best (lowest), worst (highest), or intermediate

AIC	best	intermediate	worst
SET	27	364	209
PD	8	202	390
PD($\overrightarrow{c}$)	565	34	1

Generally, in light of the mathematical fact noted in Section 2.4, the scalar property is present. Thus, the scalar property can be considered to be a transposition.

5.7 Fit by Pearson's correlation coefficient and AIC

With $c_0(s)$, $c_1(s)$, $c_2(s)$, and $c_3(s)$ fixed for each rat to the values presented in Table 2, I again calculated the fits for PD. Let PD($\overrightarrow{c}$) represent the process used to fit this revised version of the PD model to the data. In PD($\overrightarrow{c}$), since there is only one free parameter λ, its AIC value is reduced by the reduction in the number of free parameters. Incidentally, it was not possible to make a similar reduction in the number of free parameters in the SET equation using the current data and analysis; even the ratio $\frac{t_0}{b}$, the mean over the standard deviation, scattered hopelessly. Table 3 presents a comparison of the AIC values between SET, PD, and PD($\overrightarrow{c}$).

Though the mean of the correlation coefficients for PD($\overrightarrow{c}$) is lower (worse) by about 0.013 than the mean of the correlation coefficients for SET (Fig. 15), PD($\overrightarrow{c}$) has rather

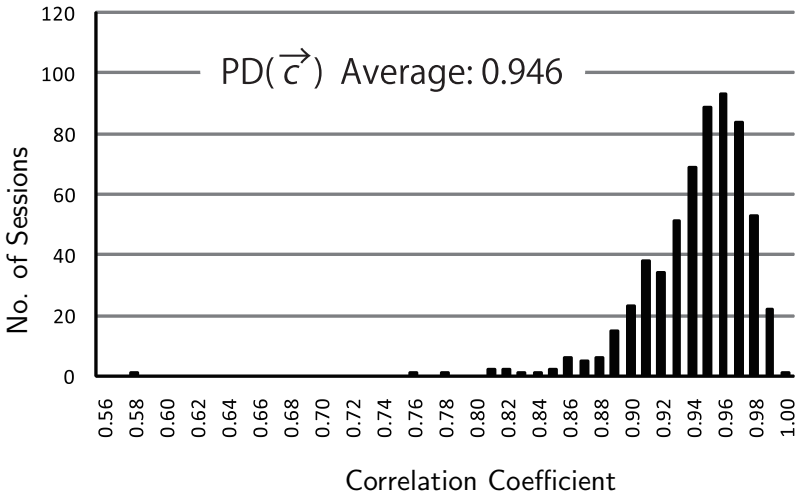

Figure 15: Frequency distribution of the correlation coefficients for the fit with PD($\overrightarrow{c}$) for 600 sessions. The mean correlation coefficient was 0.946; the method through which this mean was calculated is presented in the appendix

better AIC values than does SET (Table 3).

Obtaining the weights $c_n(s)$ using PD, I first observed that they were approximately constant. Even with this assumption which was only approximately met by the data, PD($\overrightarrow{c}$) fit the data far better, as judged by AIC values, than did SET. Therefore, I propose that PD and PD($\overrightarrow{c}$) may be useful additions to SET in the analysis of timing behavior.

5.8 Total model

"Additions to SET" in the preceding section may sound strange, because this paper might have appeared to be a rival for SET. Indeed, asymmetrically shaped graphs, such as Figure 4 in Cheng and Meck (2007), Figure 1 in Oprisan and Buhusi (2013), Figure 1 in McAuley et al. (2006) and others, turned out to be good applications for the PD model.

Symmetrically shaped graphs, such as Figure 2 in Church (1984), Figure 3 in Church et al. (1991), Figures 2 and 3 in Allman e al. (2014), Figure 4 in Oprisan and Buhusi (2013) and others, are similar, but are also still good applications for the SET model.

It is inevitable that a theme of my future research will be to apply my model to various other timing schedules, such as simultaneous temporal processing (for example, see Figure 11 in Church (1984)). Also I regard it as an important theme for future research to check whether my model is compatible and cooperative to with the striatal beat-frequency (SBF) model, as in Oprisan and Buhusi (2011; also see Figure 4 in Oprisan and Buhusi (2013)).

6 Discussion 2

6.1 Basic period of clocks, as determined by PD

In my proposed PD model, $\frac{1}{\lambda}$ (s) represents the basic period of the clock (stopwatch) that the subject used to time the PI interval. Its reciprocal, λ (1/s), represents the basic speed of the clock (stopwatch). The basic period $\frac{1}{\lambda}$ (s) of each session is shown in Figure 11, and the means of $\frac{1}{\lambda}$ (s) are shown in Figures 12 and 16.

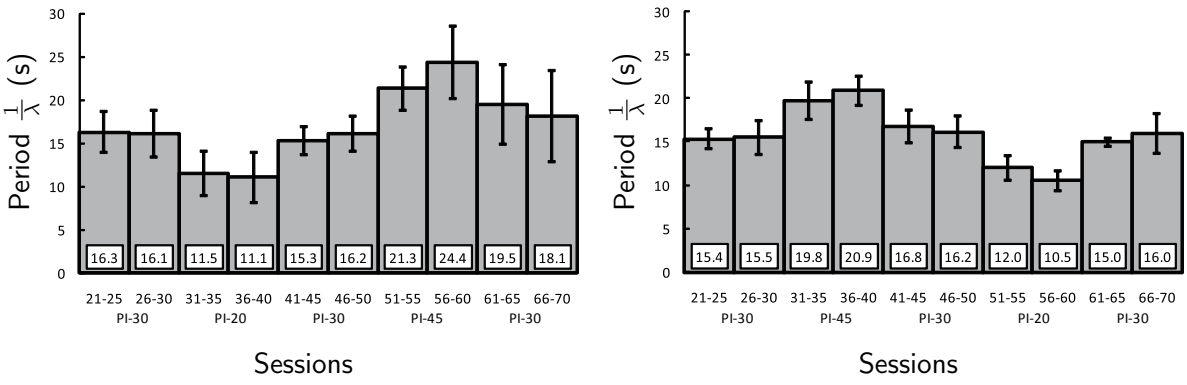

Figure 16: Mean basic clock period $\frac{1}{\lambda}$ (s), in five-session bins. Error bars present the standard deviations. The left and right panels present data from groups RatsA and RatsB, respectively

I observed that the basic clock period did not change proportionally to the FI length during the current peak procedure (Figure 12). A closer analysis revealed that the first half of each 10 sessions under the same condition was more influenced by the previous FI length than was the latter half of the sessions (Figure 16). This carry-over effect suggests

that a single clock system (stopwatch system) was involved in timing within this range (between 20 s and 45 s).

I investigated whether the peak time length and the basic period in a given condition were influenced by the PI duration during the condition immediately preceding it, and whether the sequence in which conditions were presented affected how successfully either model (SET and PD) described these data. For this analysis, I included the five sessions before and after each change in the PI length. Table 4 lists the sessions that formed part of these ascending and descending sequences. Figure 17 presents a scatter diagram of the behavioral subjective peak time t_0 that was identified after fitting SET for sessions forming part of a descending sequence (left panel), and an ascending sequence (right panel). Figure 18 presents the basic period $\frac{1}{\lambda}$ (s) that was identified after fitting PD for the same two categories of sessions.

Table 4: Sessions included in the analysis presented in Figures 17 and 18. The left half of the table presents sessions that form part of a descending sequence of PI lengths for each group, and the right half presents those that form part of an ascending sequence

Descending	From		To
RatsA	26–30	↘	31–35
	56–60	↘	61–65
RatsB	36–40	↘	41–45
	46–50	↘	51–55

Ascending	From		To
RatsA	36–40	↗	41–45
	46–50	↗	51–55
RatsB	26–30	↗	31–35
	56–60	↗	61–65

Both Figure 17 and Figure 18 show that the slope of the line fitted to the descending sequence was higher than that fitted to the ascending sequence. This indicates that

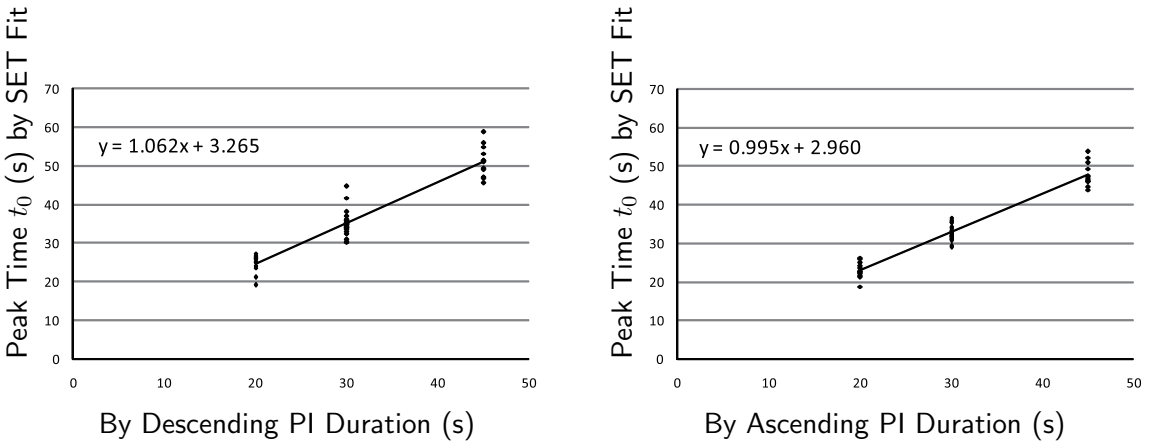

Figure 17: Scatter diagrams of the peak time t_0, identified by fitting SET to the data. Data from sessions forming part of a descending sequence are presented in the upper panel, and those forming part of an ascending sequence are presented in the lower panel. See Table 4 for the exact number of sessions of each type for each group of subjects

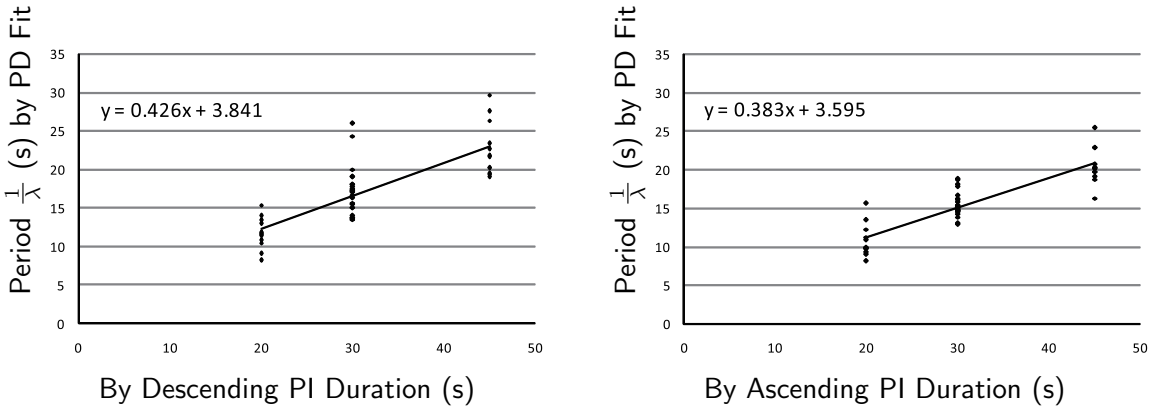

Figure 18: Scatter diagrams of the basic clock period $\frac{1}{\lambda}$, identified by fitting PD to the data. Data from sessions forming part of a descending sequence are presented in the upper panel, and those forming part of an ascending sequence are presented in the lower panel. See Table 4 for the exact number of sessions of each type for each group of subjects

changes in the PI length made in a descending sequence had a greater effect on the subjects' subjective estimates of the length of the interval than did the changes made in an ascending sequence. The emotional drive of subjects to obtain food quickly might have been expressed in this ratio.

Looking at $\frac{a_D}{a_A}$ in Table 5, we see that the sensitivity of the PD (11.2%) to the sequence in which the conditions are presented is a little greater than that of SET (6.7%),

Table 5: Slope a of the linear approximations in Figures 17 and 18 and their ratio

a	SET	PD
a_D: descending	1.062	0.426
a_A: ascending	0.995	0.383
$\frac{a_D}{a_A}$	1.067	1.112

but the variances in the parameter values identified by PD are bigger than those identified by SET, as seen in Figures 17 and 18. I will discuss this below in Section 6.2.

6.2 Peak shifts

In eq. (1) of SET, t_0 is assumed to express the peak time of a subject's subjective behavior. Figure 19 is a scatter diagram of the basic period $\frac{1}{\lambda}$ (s) of the PD fit and the peak time t_0 (s) obtained by the SET fit. The averages for five-session blocks are presented, as in Figure 16.

In Figure 19, we can clearly see three disjoint groups of points. Each group corresponds to one of the three PI durations presented. In Section 5.7 (p. 32), I conservatively compared SET and PD: "*I propose that* PD *and* PD($\overrightarrow{c}$) *may be useful additions to* SET *in the analysis of timing behavior.*" Besides the reasons presented there, Figure 19 gives an additional reason and shows why I were careful; in truth, it is necessary to include the use of SET for this study.

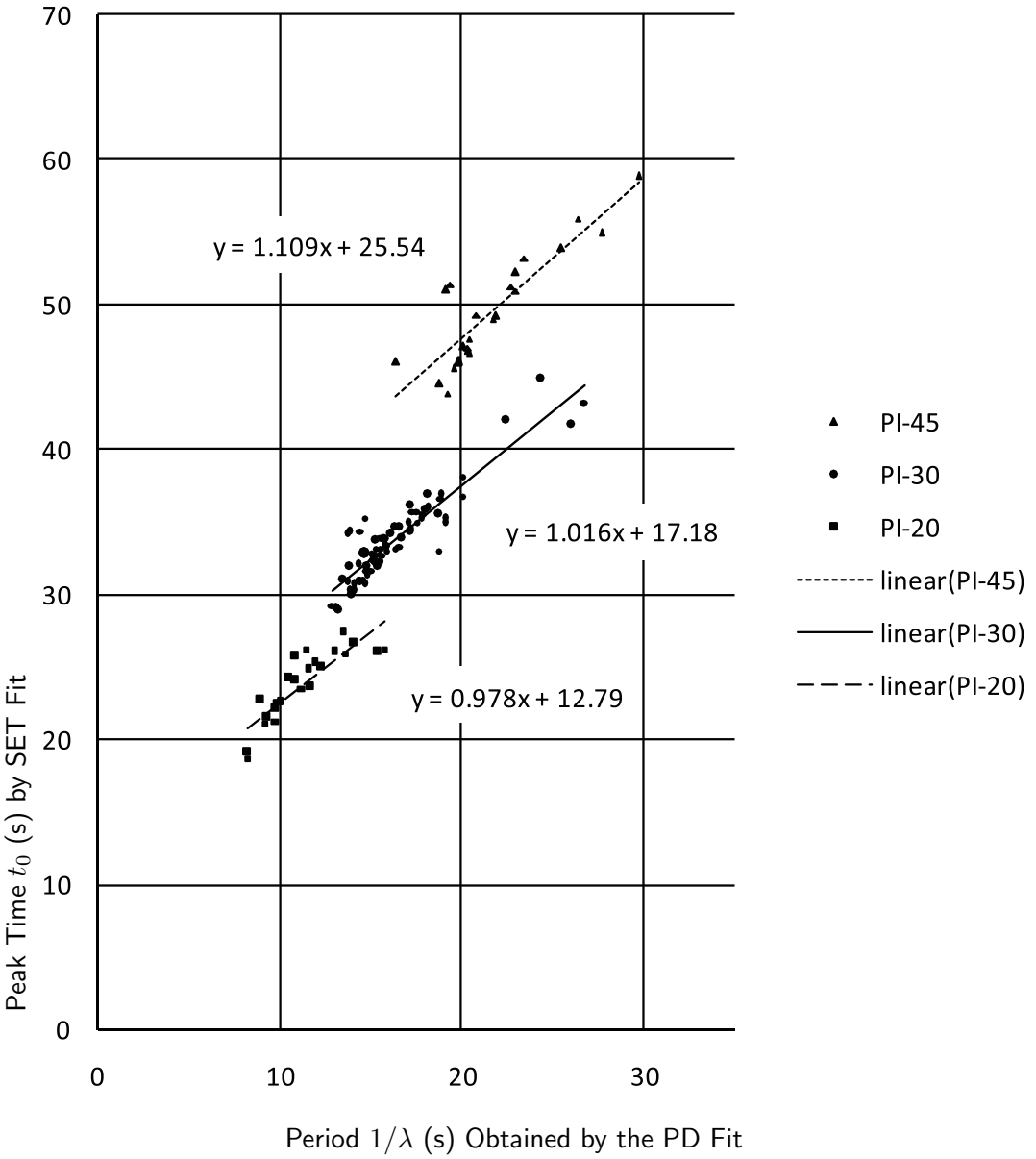

Figure 19: Scatter diagram of the period $\frac{1}{\lambda}$, based on the PD model, against the peak time t_0 identified by fitting the SET. We see three groups of points without intersection, each corresponding to one of the three PI durations that I used

The average basic clock period $\frac{1}{\lambda}$ (s) and the average clock weights $c_n(s)$ $(n = 0, 1, 2, 3)$ for PI-20 (120 sessions), PI-30 (360 sessions; the baseline), and PI-45 (120 sessions) are shown in Table 6.

The graphs of $\overline{\underline{R_s(t)}}$ for these averages are presented in Figure 20. The ratio of $c_1(s)$

and $c_3(s)$, i.e., the ratio of the weights of $X_1(t)$ and $X_3(t)$, are different for each graph. Broken curves express $c_1(s)X_1(t)$ (left) and $c_3(s)X_3(t)$ (right), which change the shape of the response graph (bold) and causes the peaks to shift (Spence 1937; Mazur 2006). Since PD features have sufficient resolution, I again propose that PD and PD($\overrightarrow{c'}$) may be useful additions to SET in the analysis of timing behavior.

The weights $c_n(s)$ calculated using PD are approximately constant. Even with this approximation, PD($\overrightarrow{c'}$) fitted slightly better than SET, as assessed by Pearson's correlation coefficient and the AIC. With this assumption, the scalar property can be considered to be a kind of transposition.

A detailed investigation, however, revealed that the weights $c_n(s)$ were not constant. Rather, they were affected by the interval length that was presented during the PI procedure. The changes in the weights reflected the shape of the response graph and caused the peaks to shift. This could be an example of where the behavior does not have the

Table 6: Average basic clock periods $\frac{1}{\lambda}$ and average clock weights $c_n(s)$ $(n = 0, 1, 2, 3)$ of PI-20, PI-30, and PI-45

	PI-20	PI-30	PI-45
$\frac{1}{\lambda}$	11.28	16.36	21.60
$c_0(s)$	0.25	0.47	0.45
$c_1(s)$	−1.81	−2.63	−2.63
$c_2(s)$	7.44	8.62	8.07
$c_3(s)$	−3.21	−3.92	−3.03

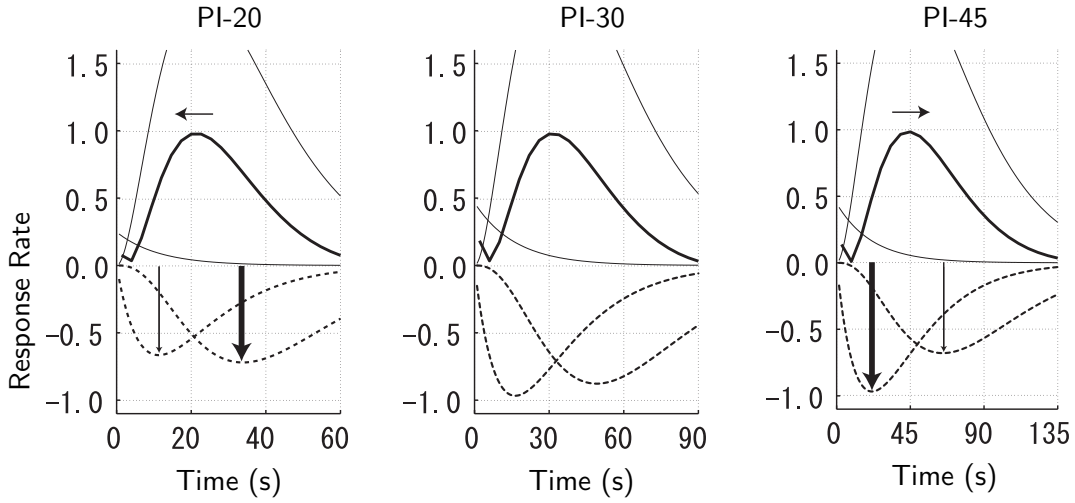

Figure 20: Graphs of $\overline{R_s(t)}$ (bold curve). Data are those presented in Table 6. The two broken curves are the graphs of $c_1(s)X_1(t)$ (left, each) and $c_3(s)X_3(t)$ (right, each), whose ratio determines the shape of $\overline{R_s(t)}$

scalar property, in an exact sense.

Rats changed both the basic periods and the weights of the clocks in order to cope with changes in the durations of the PIs. This may be why the variances in the basic period, as determined by PD, were bigger than the variances of the subjective peak times, as determined by SET (see Section 6.1).

The set of values of $c_0(s)$, $c_1(s)$, $c_2(s)$, and $c_3(s)$ shown in Table 6 represent measurements of the extent to which behavior diverged from the scalar property.

In addition to the carry-over effect discussed in Section 6.1, the transformation of the parameters in the PI procedures support the idea that each subject's clock system (stopwatch system) is unique in range, at least in when I consider durations between 20 s and 45 s. These results do not indicate the existence of separate clocks for 20 s, 30 s, and 45 s. The brain sections that become activated when a subject performs tasks that are

related to PIs in the range of 20 s to 45 s can be considered to be a set of components of a clock (stopwatch).

Appendix The mean value of the correlation coefficients

For each correlation coefficient r, after normalization by Fisher's z' transformation (r-to-z' transformation) $z' = \frac{1}{2} \ln \frac{1+r}{1-r}$, I calculated the arithmetic mean $\overline{z'}$ of z'. Then I converted back to get the mean $\overline{r}$ shown in all panels in Figs. 10 and 15.

References

[1] Akaike, H. (1974). A new look at the statistical model identification, *IEEE Transaction Automatic Control, 19*, 716–723.

[2] Allman, M. J., Teki, S., Griffiths, T. D., & Meck, W. H. (2014). Properties of the internal clock: First- and second-order principles of subjective time. *Annual Review of Psychology, 65*, 743-771.

[3] Alper, J. S., & Bridger, M. (1997). Mathematics, models and Zeno's paradoxes. *Synthese, 110*, 143–166.

[4] Beckmann, J. S., & Young, M. E. (2009). Stimulus dynamics and temporal discrimination: Implications for pacemakers. *Journal of Experimental Psychology: Animal Behavior Processes, 35*, 525–537.

[5] Buhusi, C. V., & Meck, W. H. (2005). What makes us tick? Functional and neural mechanisms of interval timing. *Nature Reviews Neuroscience, 6*(10), 755–765.

[6] Cheng, R. K., & Meck, W. H. (2007). Prenatal choline supplementation increases sensitivity to time by reducing non-scalar sources of variance in adult temporal processing. *Brain Research, 1186*, 242–254.

[7] Church, R. M. (1984). Properties of the internal clock. Annals of The New York Academy of Sciences, 423, 566–582.

[8] Church, R. M., Miller, K. D., Meck, W. H., & Gibbon, J. (1991). Symmetrical and asymmetrical sources of variance in temporal generalization. *Animal Learning & Behavior, 19*, 207–214.

[9] Church, R. M. (2003). A concise introduction to scalar timing theory. In W. H. Meck (Ed.), *Functional and Neural Mechanisms of Interval Timing* (pp. 3–22), Methods & New Frontiers in Neuroscience. Boca Raton, Florida: CRC Press LLC.

[10] Clément, A., & Droit-Volet, S. (2006). Counting in a time discrimination task in children and adults. *Behavioural Processes, 71*, 164–171.

[11] Dayan, P., & Abbott, L. F. (2001). *Theoretical Neuroscience: Computational and Mathematical Modeling of Neural Systems*. Cambridge, Massachusetts: MIT Press.

[12] Fetterman, J. G., & Killeen, P. R. (1991). Adjusting the pacemaker. *Learning and Motivation, 22*, 226–252.

[13] Fetterman, J. G., Killeen, P. R., & Hall, S. (1998). Watching the clock. *Behavioural Processes, 44*, 211–224.

[14] Gibbon, J. (1977). Scalar expectancy theory and Weber's law in animal timing. *Psychological Review, 84*, 279–325.

[15] Gibbon, J., Church, R. M., Meck, W. H. (1984). Scalar timing in memory. Annals of The New York Academy of Sciences, 423, 52–77.

[16] Gibbon J (1991). Origins of scalar timing. Learning and Motivation, 22: 3-38.

[17] Grondin, S. (2001). From physical time to the first and second moments of psychological time. *Psychological Bulletin, 127*, 22–44.

[18] Killeen, P. R. (1975). On the temporal control of behavior. *Psychological Review, 82*, 89–115.

[19] Killeen, P. R., & Fetterman, J. G. (1988). A behavioral theory of timing. *Psychological Review, 95*, 274–295.

[20] Killeen, P. R., & Taylor, T. J. (2000). How the propagation of error through stochastic counters affects time discrimination and other psychophysical judgments. *Psychological Review, 107*, 430–459.

[21] Kirkpatrick-Steger, K., Miller, S., Betti, C., & Wasserman, E. (1996). Cyclic responding by pigeons on the peak timing procedure. *Journal of Experimental Psychology: Animal Behavior Processes, 22*, 447–460.

[22] McAuley, J. D., Miller, J. P., & Pang, K. C. H. (2006). Modeling the effects of the NMDA receptor antagonist MK-801 on timing in rats. *Behavioral Neuroscience, 120*, 1163–1168.

[23] Machado, A. (1997). Learning the temporal dynamics of behavior. *Psychological Review, 104*, 241–265.

[24] Machado, A., & Guilhardi, P. (2000). Shifts in the psychometric function and their implications for models of timing. *Journal of The Experimental Analysis of Behavior, 74*, 25–54.

[25] Matell, M. S., & Meck, W. H. (1999). Reinforcement-induced within-trial resetting of an internal clock. *Behavioural Processes, 45*, 159–171.

[26] Matell, M. S., Meck, W. H., & Nicolelis, M. A. L. (2003). Interval timing and the encoding of signal duration by ensembles of cortical and striatal neurons. *Behavioral Neuroscience, 117*, 760–773.

[27] Mazur, J. E. (2006). *Learning and Behavior*. 6th ed. NJ: Prentice Hall.

[28] Meck, W. H. (1996). Neuropharmacology of timing and time perception. *Cognitive Brain Research, 3*, 227–242.

[29] Meck, W. H. (2006). Neuroanatomical localization of an internal clock: a functional link between mesolimbic, nigrostriatal, and mesocortical dopaminergic systems. *Brain Research, 1109*, 93–107.

[30] Oprisan, S. A., & Buhusi, C. V. (2011). Modeling pharmacological clock and memory patterns of interval timing in a striatal beat-frequency model with realistic, noisy neurons. *Frontiers in Integrative Neuroscience, 5*: 52.

[31] Oprisan, S. A., & Buhusi, C. V. (2013). Why noise is useful in functional and neural mechanisms of interval timing? *BMC Neuroscience, 14*: 84.

[32] Roberts, S. (1981). Isolation of an internal clock. *Journal of Experimental Psychology: Animal Behavior Processes, 7*, 242–268.

[33] Saigusa, T., Tero, A., Nakagaki, T., & Kuramoto, Y. (2008). Amoebae anticipate periodic events. *Physical Review Letters, 100*(1), 018101.

[34] Spence, K. W. (1937). The differential response in animals to stimuli varying within a single dimension. *Psychological Review, 44*, 430–444.

[35] Staddon, J. E. R., & Higa, J. J. (1999). Time and memory: Towards a pacemaker-free theory of interval timing. *Journal of The Experimental Analysis of Behavior, 71*, 215–251.

[36] Vlastos, G. (1967). Zeno of Elea, In *The Encyclopedia of Philosophy, 8* (pp. 369–379), New York: Macmillan.

[37] Yi, L. (2007). Applications of timing theories to a peak procedure. *Behavioural Processes, 75*, 188–198.

[38] Zentall, T. R. (2006). Timing, memory for intervals, and memory for untimed stimuli: The role of instructional ambiguity. *Behavioural Processes, 71*, 88–97.